Recognition and Discrimination of Gases by the Oxygen-Sensing Signal Transducer Protein HemAT As Revealed by FTIR Spectroscopy†

Eftychia Pinakoulaki,‡ Hideaki Yoshimura,§ Shiro Yoshioka,§ Shigetoshi Aono,§ and Constantinos Varotsis*,‡

Department of Chemistry, University of Crete, 71409 Heraklion, Crete, Greece, and Okazaki Institute for Integrative Bioscience, National Institutes of Natural Sciences, Okazaki, Aichi 444-8787, Japan

Received March 1, 2006; Revised Manuscript Received May 10, 2006

ABSTRACT: The determination of ligand binding properties is a key step in our understanding of gas sensing and discrimination by gas sensory proteins. HemAT is a newly discovered signal transducer heme protein that recognizes O_2 and discriminates against other gases such as CO and NO. We have used FTIR spectroscopy on CO- and NO-bound sensor domain HemAT and sensor domain distal mutants Y70F, T95A, R91A, and L92A to gain insight into the structure of the iron-bound ligand at ambient temperature. These mutations were designed to perturb the electrostatic field near the iron-bound gaseous ligand and also allow us to investigate the communication pathway between the distal residues of the protein and the heme. We show the formation of both H-bonded and non-H-bonded conformations in the CO-bound forms. In addition, we report the presence of multiple conformations in the NO-bound forms. Such distal H-bonding is crucial for ligand binding and activation by the heme. The comparison of the O_2, NO, and CO data demonstrates that Thr95 and Tyr70 are crucial for ligand recognition and discrimination and, thus, for specific sensing of gases, and L92 is crucial for controlling the conformational changes of the Thr95 and Tyr70 residues upon NO binding.

HemAT[1] is a newly discovered signal transducer heme protein that detects O_2 and transmits the signals through conformational changes to histidine kinase (*1*−*7*). The crystal structure of HemAT has revealed that the protein is a homodimer (*3*). Little is known about the dynamics of signal transduction by transmembrane chemoreceptors (*2*−*7*). Six-coordinate O_2-bound HemAT-Bs forms have been recently reported, suggesting the involvement of distal residues T95 and Y70 in regulating O_2 binding (*6*, *7*). In addition, L92 has been implicated in the concerted movement of T95 and Y70 for the formation of the distinct forms of the O_2-bound HemAT (*6*, *7*). In an effort to further characterize the ligand binding properties of HemAT, we have used FTIR spectroscopy to characterize the CO- and NO-bound ligands with sensor and full-length HemAT. Distal protein mutants R91A, T95A, Y70F, and L92A upon CO and NO binding have also been characterized. These mutations were designed to perturb the electrostatic field near the iron-bound gaseous ligand and also to allow us to investigate the communication pathway between the distal residues of the protein and the heme. The comparison of the O_2, NO, and CO data demonstrates that T95 and Y70 are crucial for ligand recognition and discrimination and, thus, for specific sensing of gases. In addition, the data indicate that L92 controls the conformational changes of T95 and Y70 upon NO binding. Such specific recognition and discrimination of gases are profoundly important in our understanding of intramolecular signal transduction by HemAT.

MATERIALS AND METHODS

Expression and Purification of HemAT. HemAT was expressed in *Escherichia coli* BL21(DE3) under the control of the T7 promoter in the pET24(+) vector (Novagen). HemAT was obtained as a C-terminal six-His-tagged protein. All mutants were prepared using the QuikChange site-directed mutagenesis kit (Stratagene). The *E. coli* BL21(DE3) harboring the expression vector was grown aerobically at 37 °C for 4 h in TB medium containing 30 μg/mL kanamycin. The expression was induced by adding 1 mM isopropyl 1-thio-D-galactopyranosids, and then the cultivation continued at 22 °C for 18 h. The cells were harvested by centrifugation at 4000*g* and stored at −78 °C until they were used. Purification of HemAT was carried out as follows. The cells were thawed and resuspended in 50 mM Tris-HCl buffer (pH 8.0) containing 15 mM glycine and 1 M NaCl and then were broken by sonication. The resulting suspension was centrifuged at 28 000 rpm for 20 min, and the supernatant was loaded on a Ni-charged HiTrap chelating column (Amersham). After the column had been washed with 50 mM Tris-HCl buffer (pH 8.0) containing 15 mM glycine and then with 1 M NaCl and 50 mM Tris-HCl buffer (pH 8.0), the adsorbed proteins were eluted with 50 mM Tris-HCl buffer (pH 8.0) containing 100 mM imidazole. The fractions containing HemAT were combined and loaded onto a HiTrap Q HP column (Amasham). The

† This work was supported by the GSRT and the Ministry of Education (C.V.) and by Grants-in-Aid for Scientific Research B (16370065) from the Ministry of Education, Science, Sports and Culture, Japan (S.A.).

* To whom correspondence should be addressed. Telephone: +30-2810393653. Fax: +30-2810393601. E-mail: varotsis@edu.uoc.gr.

‡ University of Crete.

§ National Institutes of Natural Sciences.

[1] Abbreviations: HemAT, heme-based aerotactic transducer; Mb, myoglobin; FTIR, Fourier transform infrared.

10.1021/bi0604072 CCC: $33.50
Published on Web 06/06/2006

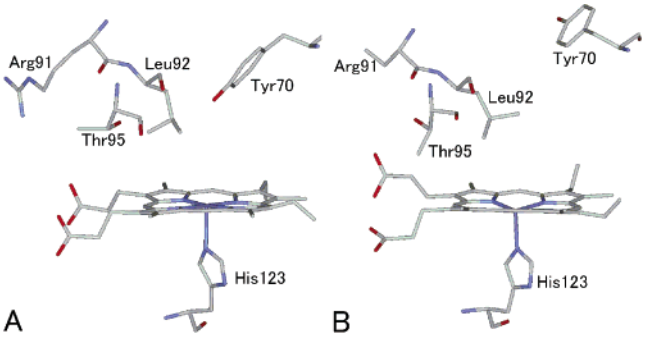

FIGURE 1: Asymmetric dimer active site of the unligated HemAT sensor domain (PDB entry 1OR6) (*3*).

column was washed with 50 mM Tris-HCl buffer (pH 8.0) containing 100 mM NaCl, and then HemAT was eluted by increasing the concentration of NaCl in 50 mM Tris-HCl buffer (pH 8.0).

FTIR Spectroscopy. Dithionite-reduced samples were exposed to 1 atm of CO (1 mM) in an anaerobic cell to prepare the carbonmonoxy adduct and loaded anaerobically into a cell with CaF_2 windows and a 0.025 mm spacer. CO gas was obtained from Messer, and isotopic CO (^{13}CO) was purchased from Isotec. The nitrosyl HemAT samples were prepared upon exposure of the oxidized samples to 1 atm of NO. NO gas was obtained from Messer. The pD solutions prepared in D_2O buffers were measured by using a pH meter and assuming pD = pH (observed) + 0.4. FTIR spectra were obtained from 500 μM samples with a Bruker Equinox 55 FTIR spectrometer equipped with a liquid nitrogen-cooled mercury cadmium telluride detector. The FTIR spectra were obtained as difference spectra, using the buffer as background, and each spectrum is the average of 1000 scans. Optical absorbance spectra were recorded before and after FTIR measurements to assess sample stability with a Perkin-Elmer Lamda 20 UV−visible spectrometer.

RESULTS

Figure 1 shows a schematic presentation of the asymmetric dimer active site of the unligated HemAT sensor domain (PDB entry 1OR6) (*3*). The absorption spectrum of CO-bound HemAT is similar to those reported previously (*2*, *4*) (data not shown). We detect two modes in the FTIR spectrum of the CO-bound HemAT (Figure 2A). We assign the ν_{CO} of HemAT on the basis of the ν_{CO} of Mb observed at 1910−1930 cm^{-1} (strong H-bonding interaction), 1940−1950 cm^{-1} (moderate H-bonding interaction), and 1960−1970 cm^{-1} (neutral) (*8*). Therefore, we assign the major band (*2*, *4*) at 1967 cm^{-1} (neutral) and the minor band (strong H-bonding interaction) at 1928 cm^{-1} to the C−O modes of the heme Fe−CO complex. In the ^{13}CO-bound complex, these modes shift to 1923 and 1877 cm^{-1}, respectively (Figure 2B). The detection of the major band has been reported in the past (*2*, *4*), but the strong H-bonding conformer is reported for the first time. The frequencies of the CO modes are independent of H_2O−D_2O exchange (Figure 2C,D). In the spectra of the T95A (Figure 2E) and R91A (Figure 2F) mutants in addition to the major C−O mode at 1967 cm^{-1}, the strong-H-bonding conformer at 1931 cm^{-1} is present. In the spectrum of the L92A mutant (Figure 2G), the C−O mode is observed at 1969 cm^{-1} but the strong H-bonding conformer at 1931 cm^{-1} is absent. Interestingly, in the Y70F mutant (Figure 2H), the

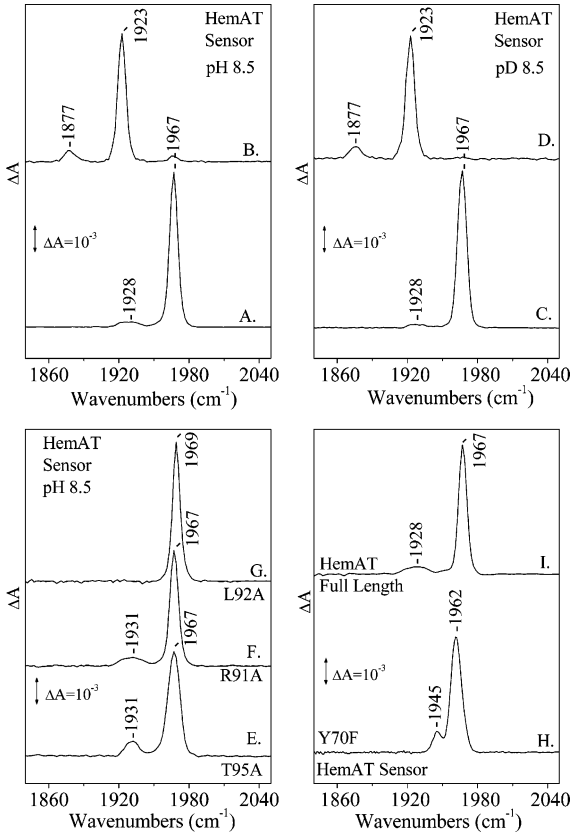

FIGURE 2: FTIR spectra of CO-bound HemAT proteins at ambient temperature. The reduced samples with bound $^{12}C^{16}O$ are shown in traces A (pH 8.5, sensor domain) and C (pD 8.5, sensor domain). The reduced samples with bound $^{13}C^{16}O$ are shown in traces B (sensor domain, pH 8.5) and D (sensor domain, pD 8.5). The reduced samples with bound $^{12}C^{16}O$ are shown in traces E (T95A, sensor domain), F (R91A, sensor domain), G (L92A, sensor domain), H (Y70F, sensor domain), and I (full length, wild type). The spectral resolution used for the FTIR measurements was 4 cm^{-1} for all spectra.

C−O mode observed at 1962 cm^{-1} is 5 cm^{-1} lower than that observed in the wild-type sensor domain protein, and the presence of the 1945 cm^{-1} mode indicates the formation of a modest H-bonding conformer. In the full-length protein (Figure 2I), both CO modes are the same as those observed in the sensor domain protein (Figure 2A,C).

The absorption spectrum of the NO-bound oxidized WT sensor HemAT depicted in Figure 3B shows transitions at 418, 533, and 567 nm. No characteristic transitions of a six- or five-coordinate ferrous nitrosyl HemAT are present. The FTIR spectra of the NO-bound oxidized WT sensor and of the distal mutants of HemAT at pH/pD 8 are displayed in Figure 4A−F. The band fitting analyses located the center of the NO Gaussian bands at 1903, 1912, 1920, and 1927 cm^{-1} as delineated by the green lines. The 1903 and 1920 cm^{-1} vibrations are similar to those obtained in Mb (*9*, *10*) at 1907 and 1922 cm^{-1}, respectively, and similar to those found in other NO-bound heme proteins (*11*−*14*).

In Mb, the stability of the heme Fe−NO complex depends on the protonation of the distal His. At low pH, the distal His swings out into the solvent stabilizing the $Fe^{+}{=}N{=}O$ structure (ν_{NO} = 1907 cm^{-1}) (*9*, *10*, *12*). If the lone pair of the distal His is located on the O atom of the bound NO, then the $Fe{-}N{\equiv}O^{+}$ structure is stabilized, and ν(NO) is increased (ν_{NO} = 1921 cm^{-1}). The ν(NO) at 1903 cm^{-1}

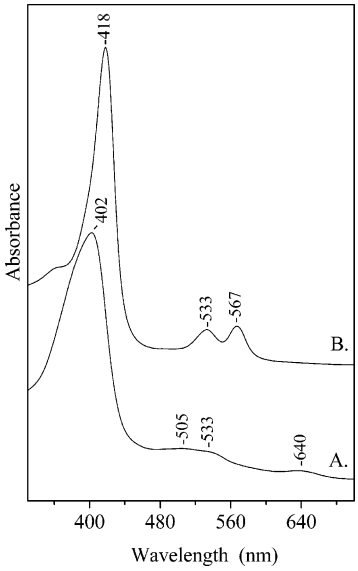

FIGURE 3: Absorption spectra of oxidized wild-type sensor domain HemAT (A) and the ferric NO-bound form (B).

we observe in HemAT is consistent with a linear heme Fe−N−O unit in which substantial donation of charge from NO to heme Fe^{3+} has occurred, resulting in a species with considerable NO^+ character, and an elevated ν(NO) stretching frequency, as compared to those of free NO (1875 cm^{-1}) and ferrous NO (1590−1681 cm^{-1}) (*15*, *16*). The linear $Fe^{2+}-N{\equiv}O^+$ character means that partial charge transfer from NO to Fe^{3+} occurs during the bonding process. On the basis of the similarities of the NO frequencies between HemAT and Mb, we assign the 1903 and 1912 cm^{-1} bands to conformers exhibiting no interaction with the distal residues and the 1920 and 1927 cm^{-1} bands to conformers exhibiting interaction with the distal residues. In D_2O (Figure 4B), the frequencies of the bound NO and the ratio of the conformers exhibiting no interaction with the distal residues to those exhibiting interaction are similar to those obtained in H_2O. In R91A (Figure 4C), no significant changes are observed with the exception of the increased intensity of the 1927 cm^{-1} band at the expense of the 1920 cm^{-1} band. This indicates that R91 has little interaction with the bound NO. In T95A (Figure 4D), only the conformers exhibiting no interaction with the distal residues at 1901 and 1911 cm^{-1} are present, demonstrating the involvement of T95 in the formation of the 1920 and 1927 cm^{-1} conformers. In Y70F (Figure 4E), both types of conformers at 1899 and 1918 cm^{-1} are detected. Finally, in L92A (Figure 4F), only the conformers exhibiting interaction at 1918 and 1928 cm^{-1} are observed.

DISCUSSION

CO Binding. The presence of the 1928/1931 cm^{-1} (strong H-bonding conformer) and 1945 cm^{-1} (modest H-bonding conformer) modes in the sensor, R91A, T95A, and Y70F mutants and in full-length HemAT indicate the existence of modest and strong H-bonding conformers, as found in the O_2-bound form (*6*). The results from the CO-bound HemAT experiments indicate that the CO-bound ligand retains the H-bonded and non-H-bonded conformations because all frequencies of the CO modes in the wild-type sensor protein are independent of H_2O-D_2O exchange. The absence of the strong H-bonding conformer in L92 indicates that this residue significantly perturbs its formation. In addition, Y70 regulates the H-bonding interactions in the distal protein environment upon CO binding as shown by the formation of the modest H-bonding conformer at 1945 cm^{-1} and the neutral conformer at 1962 cm^{-1} in the Y70F protein. It should be noted that the 1945 cm^{-1} band was not observed previously in the Y70F protein (*4*). Finally, on the basis of the similarity of the CO-bound spectra of T95A and wild-type sensor proteins, we conclude that no communication pathway exists between

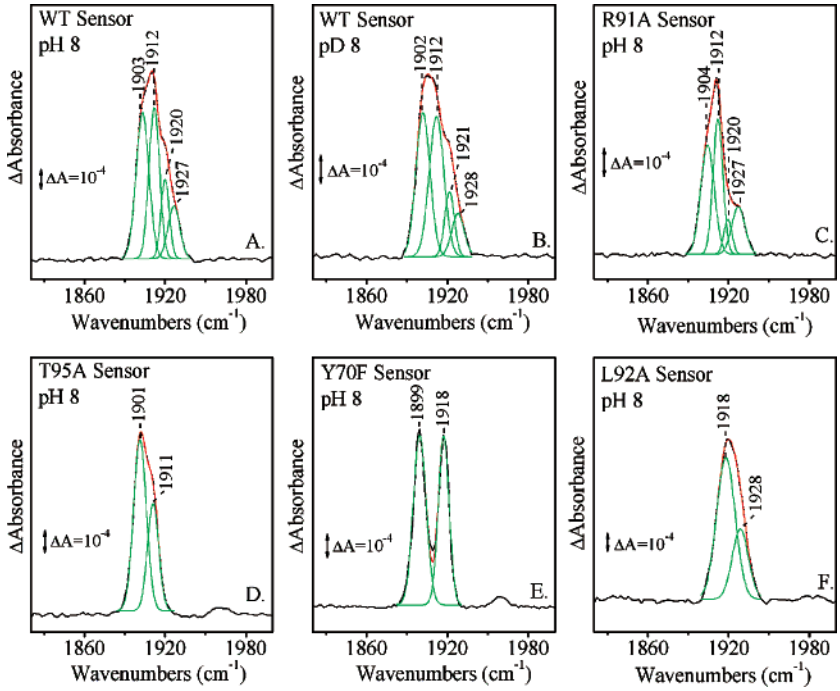

FIGURE 4: FTIR spectra of NO-bound sensor domain HemAT at pH 8 (A) and pD 8 (B), NO-bound R91A (C), NO-bound T95A (D), NO-bound Y70F (E), and NO-bound L92A (F). The green lines are the band fitting components, and the red lines are the sums of the component bands.

T95 and the CO bound to the heme Fe, as opposed to that for the O_2-bound HemAT (*6*).

NO Binding. The NO data suggest that T95 contributes, as opposed to CO-bound but like O_2-bound HemAT (*6*), to the communication of the NO bound to the heme with the distal protein environment through the formation of conformations exhibiting interaction with the distal environment. In addition, Y70 is involved in the interactions of the bound ligand with the distal environment through the formation of only one of two conformers exhibiting interaction (1927 cm^{-1}), as opposed to O_2 (*6*) but similar in this case to that of CO-bound HemAT. The absence of the conformers exhibiting no interaction in the L92A protein indicates its involvement in regulating the necessary structural changes of T95 and Y70 for the formation of the multiple conformations.

Ligand Discrimination and Recognition. The data presented here and those previously reported (*2*, *4*−*7*) suggest that although the heme cavity recognizes ligands such as O_2, NO, and CO the conformational changes induced in the protein distal site are not similar, and thus, only O_2 alters the distal site in such a way that the conformational changes are transmitted to the effector domain. The behavior of R91 upon ligand binding indicates that it is not involved in any kind of structural changes that influence the ligand recognition and discrimination. The behavior of T95 and Y70 upon binding of O_2, CO, and NO to the heme Fe produces distinct conformations indicating that they are the major contributors in ligand recognition and discrimination. On the other hand, L92 induces the necessary structural changes to T95 and Y70 for the formation of the NO-bound conformations exhibiting interaction with the distal residues and the conformations exhibiting no interaction. For the CO-bound ligand, L92 generates the necessary structural changes to the distal environment for maintenance of the H-bonded conformer. This study demonstrates the unique specificity and tuning of the distal amino acid residues of HemAT in constructing the necessary conformational changes toward ligand recognition. Such specific recognition and discrimination of iron-bound gaseous ligands by the distal protein environment are crucial to the intramolecular signal transduction by HemAT.

REFERENCES

1. Hou, S., Larsen, R. W., Boudko, D., Riley, C. W., Karatan, E., Zimmer, M., Ordal, G. W., and Alam, M. (2000) Myoglobin-like aerotaxis transducers in Archaea and Bacteria, *Nature 403*, 540−547.
2. Aono, S., Kato, T., Matsuki, M., Nakajima, H., Ohta, T., Uchida, T., and Kitagawa, T. (2002) Resonance Raman and ligand binding studies of the oxygen-sensing signal transducer protein HemAT from *Bacillus subtilis*, *J. Biol. Chem. 277*, 13528−13538.
3. Zhang, W., and Phillips, G. (2003) Structure of the oxygen sensor in *Bacillus subtilis*: Signal transduction of chemotaxis by control of symmetry, *Structure 11*, 1097−1110.
4. Zhang, W., Olson, J. S., and Phillips, G. (2005) Biophysical and kinetic characterization of HemAT, an aerotaxis receptor from *Bacillus subtilis*, *Biophys. J. 88*, 2801−2814.
5. Aono, S., Nakajima, H., Ohta, T., and Kitagawa, T. (2004) Resonance Raman and ligand binding analysis of the oxygen-sensing signal transducer protein HemAT from *Bacillus subtilis*, *Methods Enzymol. 381*, 618−628.
6. Ohta, T., Yoshimura, H., Yoshioka, S., Aono, S., and Kitagawa, T. (2004) Oxygen-sensing mechanism of HemAT from *Bacillus subtilis*: A resonance Raman spectroscopic study, *J. Am. Chem. Soc. 126*, 15000−15001.
7. Ohta, T., and Kitagawa, T. (2005) Resonance Raman investigation of the specific sensing mechanism of a target molecule by gas sensory proteins, *Inorg. Chem. 44*, 758−769.
8. Li, T., Quillin, M. L., Phillips, G. N., and Olson, J. S. (1994) Structural determinants of the stretching frequency of CO bound to myoglobin, *Biochemistry 33*, 1433−1446.
9. Tomita, T., Haruta, N., Aki, M., Kitagawa, T., and Ikeda-Saito, M. (2001) UV resonance Raman detection of a ligand vibration on ferric nitrosyl heme proteins, *J. Am. Chem. Soc. 123*, 2666−2667.
10. Miller, L. M., Pedraza, A. J., and Chance, M. R. (1997) Identification of conformational substates involved in nitric oxide binding to ferric and ferrous myoglobin through difference Fourier transform infrared spectroscopy (FTIR), *Biochemistry 36*, 12199−12207.
11. Pinakoulaki, E., Gemeinhardt, S., Saraste, M., and Varotsis, C. (2002) Nitric-oxide reductase. Structure and properties of the catalytic site from resonance Raman scattering, *J. Biol. Chem. 277*, 23407−23413.
12. Stavrakis, S., Pinakoulaki, E., Urbani, A., and Varotsis, C. (2002) Fourier transform infrared evidence for a ferric six-coordinate nitrosylheme b_3 complex of cytochrome cbb_3 oxidase from *Pseudomonas stutzeri* at ambient temperature, *J. Phys. Chem. B 106*, 12860−12862.
13. Wang, Y., and Averill, B. (1996) Direct observation by FTIR spectroscopy of the ferrous heme-NO^+ intermediate in reduction of nitrite by a dissimilatory heme cd_1 nitrite reductase, *J. Am. Chem. Soc. 118*, 3972−3973.
14. Ding, X. D., Weichsel, A., Andersen, J. F., Shokhireva, T. K., Balfour, C., Pierik, A. J., Averill, B. A., Montfort, W. R., and Walker, F. A. (1999) Nitric oxide binding to the ferri- and ferroheme states of nitrophorin 1, a reversible NO-binding heme protein from the saliva of the blood-sucking insect, *Rhodnius prolixus*, *J. Am. Chem. Soc. 121*, 128−138.
15. Pinakoulaki, E., Ohta, T., Soulimane, T., Kitagawa, T., and Varotsis, C. (2005) Detection of the His-heme Fe^{2+}-NO species in the reduction of NO to N_2O by ba_3-oxidase from *Thermus thermophilus*, *J. Am. Chem. Soc. 127*, 15161−15167.
16. Pinakoulaki, E., Stavrakis, S., Urbani, A., and Varotsis, C. (2002) Resonance Raman detection of a ferrous five-coordinate nitrosylheme b_3 complex in cytochrome cbb_3 oxidase from *Pseudomonas stutzeri*, *J. Am. Chem. Soc. 124*, 9378−9379.

BI0604072